

Interpolation of Orientation : Axiomatic Approach and Applications

Anatole Chessel
IFREMER/LASAA
BP 70, Technopole Brest-Iroise
28280, Plouzane, France
achessel@ifremer.fr

Frederic Cao
IRISA/VISTA
Campus de Beaulieu
35041, Rennes, France
fcao@irisa.fr

Ronan Fablet
IFREMER/LASAA
BP 70, Technopole Brest-Iroise
28280, Plouzane, France
rfablet@ifremer.fr

May 30, 2006

Abstract

This paper develops an axiomatic approach of vector field orientation, seen as angles on the unit circle. Two operators will be singled out: the curvature operator, appearing in total variation minimisation for image restoration and inpainting/disocclusion, as a direct solution and the Absolutely Minimizing Lipschitz Extension (AMLE), already known as a robust and coherent scalar image interpolation technique, if we relax slightly the axioms. Numerical results are presented on real and artificial images using a multiresolution finite differences scheme. The computed field is shown to be able to extend geometrical information from images in accordance with the human perception of edges. First applications are shown, including a Fast Marching contour extraction algorithm and a LIC-based smoothing method.

1 Introduction

The strength of human vision is known to be its ability to work with heterogeneous visual cues and combine them to reconstruct a global organisation of the visual stimuli out of local features. The long term goal of Computer vision is to achieve the same degree of integration and robustness. If the local/global interaction has gathered much work, the heterogeneous visual cues part of that program, however, has seldom been emphasised upon. It is as problematic: how to go beyond purely contrast-based imaging to include geometrical information?

Detecting what we intuitively call "edges" is a first step towards low level feature extraction and integration and has been the focus of a lot of work since the beginning of computer vision ([6, 11, 12] etc...). But as noted by psycho-visual experiments and models [16], that concept has appeared to be more difficult to define than simply "contrasted image part". Psychovision experiments by the Gestaltists [16, 33] has given us an acute and unified framework to analyse those effects, and many grouping laws are often involved in the recognition of what we call an edge. The so-called subjective contour effect in particular let us see edges which are strictly speaking not even actually present. It uses amodal completion (reconstruction of occluded edges due to the 2D projection of a 3D world) and modal completion (leading to *illusory contour*, where the object and the background have the same color). In both cases it rely on a curve interpolation process of unknown data according to the input.

The main origin for those subjective contours is the good continuation principle, which states that if two edgels (edge elements, i.e. points together with the orientation of the curve which should pass through it) are not too far apart and have compatible directions, we tend to see the curve to which they are both tangent as an edge. Many studies have aimed at computationally implementing this phenomenon. To this end, it is generally assumed that a filter has given us an image of edgels from which we want to extract the curves. Two classical approaches are the curve detector of Parent and Zucker [25], which uses a discrete co-circularity measure to extract potentially interesting point, and Sha'ashua and Ullman saliency network [29], where dynamic programming is used to exhaustively search for the "best" curves under curvature minimisation and length maximisation constraints. More recently, interesting approaches are Medioni's tensor voting [19, 20], where curves emerge from votes of sparse edgels, and Zweck and al. stochastic completion fields [34], an Euclidean group invariant implementation of the advection-diffusion model of Mumford [21].

The good continuation principle states conditions on tangent vectors, and most of the approaches mentioned earlier rely, explicitly or not, on vector or orientation fields. The present work aims at finding out the most invariant interpolation methods based on partial differential equations (PDEs).

Given a set of edgels, what are the most invariant and stable ways to reconstruct an orientation field in the whole plan? Because orientations live on the unit circle, an everywhere smooth interpolation is not always possible, due to global topological arguments. However, if we now use local arguments, a analysis similar to [1, 7] is possible and leads also to similar necessary conditions, showing that only very few differential operators have good properties. Since the functions which will be considered in this paper are vector valued or have values in the unit circle, only little is known about existence, uniqueness or classification of the singularities of the solutions to equations we single out. This contribution is an insight of what could be those results and their interest from a low-level vision point of view.

Related problems include image inpainting and restoration, and the operators described here are also applied in those cases. In particular, recent development extended them to the case of non-scalar images (vector or tensor

valued images) [4, 17, 23]. The aim however is different, as this work does not seek to recover the image itself, but an orientation field that would capture its geometrical features.

Section 2 states some generalities about interpolating angle, and in particular that singularities are often unavoidable. Section 3 is devoted to the actual axiomatic approach. The next section presents in more details the two singled out operators. The numerical implementation is described in Section 5, along with the multiresolution algorithm used for initialisation. Section 6 present numerical experiments on natural and artificial images. Two basic applications of such a dense geometry driven orientation field are shown in the last section.

2 Interpolating Angles

Let $\Omega \subset \mathbb{R}^2$ and $\partial\Omega$ its boundary. Let S^1 be the unit circle of \mathbb{R}^2 . We consider the *extension problem*: knowing $I : \partial\Omega \rightarrow S^1 \subset \mathbb{R}^2$, how to extend I to the whole domain Ω ? To work in S^1 we need a parameterisation, in order to handle numerically geometrical data. Let the bijective function $\phi : U \subset S^1 \rightarrow V \subset \mathbb{R}$ be such a parameterisation. The circle S^1 represents angular data modulo 2π . In addition, we may also consider the directions of unoriented lines (*i.e.* angles modulo π). All the argumentation below will apply to both cases.

2.1 Topological Restriction

The first problem we encounter when extending vectors as opposed to scalars, is that singularities in the field may be unavoidable. Given a data to be interpolated when can we hope for a singularity free extension? A necessary and sufficient condition is the following.

Proposition 1. *Let f be a continuous vector field over $\partial\Omega$. There exists a continuous extension of f to Ω if and only if f satisfies condition C,*

$$\exists \alpha \in S^1, \alpha \notin f(\partial\Omega), \tag{C}$$

that is to say only if f is not surjective.

These topological results mean that a singularity free extension is impossible for orientation field when the bounding data cover the whole unit circle. This classical result is equivalent to the Brouwer fixed point theorem [14]. In all the following theoretical consideration, condition (C) is assumed to be true.

2.2 A Fundamental Ambiguity

The parameterisation ϕ is not unique and an extension method has to be as independent from it as possible. Unfortunately, the periodicity of S^1 leads to an unavoidable ambiguity in interpolation. Let ψ be another parameterisation $\psi : U' \subset S^1 \rightarrow V' \subset \mathbb{R}$. In the axiomatic developed in Section 3, the case of a parameterisation change $g = \psi \circ \phi^{-1}$ will be handled. But this assumes that

$U \cap U'$ is a compact, that the two parameterisation have compatible domains in S^1 .

Let f be a continuous vector field over $\partial\Omega$. If $f(\partial\Omega) \subset S^1$ have $n > 1$ connected components, due to the periodicity of S^1 there exists n ways of choosing the compact U in which the interpolation is done (see Fig 1 left). This choice is equivalent to choosing the point left out of the parameterisation, thus it gives rise to non-equivalent extension. For example Fig. 1 right, the extension can either go through zero or $\frac{\pi}{2}$.

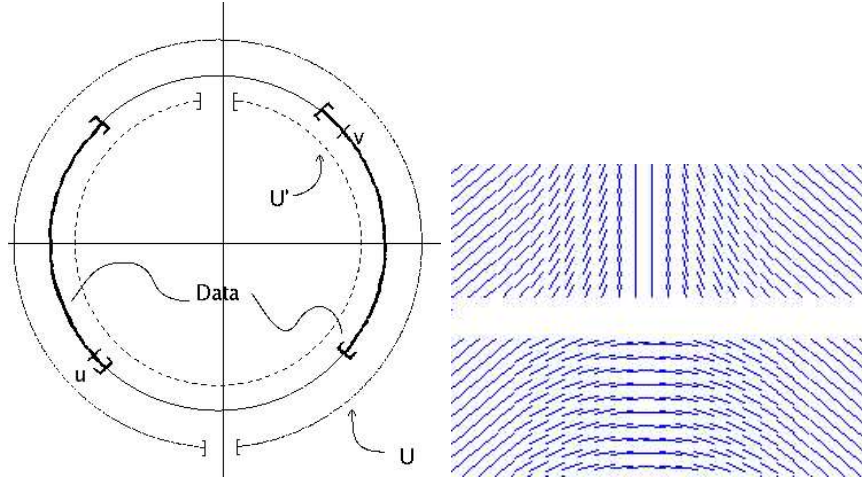


Figure 1: Ambiguity of interpolation of angle. Left: there are two ways of going from u to v , one in U , the other in U' (modulo 2π). Right: example when $u - v = \pi/2$ (modulo π for clarity)

In the following theoretical consideration, such a choice is implicitly assumed once and for all. Numerically however, iterative scheme are used and they may yield different final result depending on the initialisation. Moreover, the topological condition (C) might not be fulfilled in practice for the whole domain but only in sub-domains. In that case, the choice of the parameterisation at a point depends on its neighbourhood. A possible workaround is a multiresolution scheme, as detailed in Section 5.

3 Axiomatic Approach

This section details the axiomatic approach exploited to define operators for the interpolation of orientation field.

Let Γ be a continuous Jordan curve bounding a simply connected domain Ω . We look for an extension operator E , which associates with each directional data $\theta_0 : \Gamma \rightarrow S^1$ a unique extension $E(\Gamma, \theta_0)$. Throughout all the discussion

to follow, it is assumed that θ_0 satisfies global condition (C). The set of all those functions will be denoted by $\mathcal{F}(\Gamma)$. As previously stressed, it is necessary to parameterise S^1 to deal with numerical functions. A slight difficulty arises, since it is not possible to describe the whole circle by a unique chart. Let ϕ be such a local parameterisation, that is to say, a bijective function $U \rightarrow V$, where U is an open subset strictly included in S^1 and V an open subset of \mathbb{R} . Let us now consider the extension operator E_ϕ interpolating real valued boundary data u , defined by $E_\phi(\Gamma, u) = \phi \circ E(\Gamma, \phi^{-1} \circ u)$. Since $E_\phi(\Gamma, u)$ is a numerical function, it is easier to formulate conditions on the operator E_ϕ . However, since the parameterisation ϕ is arbitrary, the result should be independent on the parameterisation and condition on E_ϕ should stand for any ϕ .

Following [7], E_ϕ is required to satisfy the following axioms:

Axiom (A1): Comparison principle *Let $\theta_1, \theta_2 \in \mathcal{F}(\Gamma)$ such that they can be described by a common chart ϕ . Then $\phi(\theta_1) \geq \phi(\theta_2)$ implies*

$$E_\phi(\Gamma, \phi(\theta_1)) \geq E_\phi(\Gamma, \phi(\theta_2)). \quad (1)$$

Axiom (A2): Stability principle *Let $\Gamma \in \mathcal{C}$, $\theta_0 \in \mathcal{F}(\Gamma)$, and $\Gamma' \in \mathcal{C}$ such that $D(\Gamma') \subseteq D(\Gamma)$. Then,*

$$E(\Gamma', E(\Gamma, \theta_0)|_{\Gamma'}) = E(\Gamma, \theta_0)|_{D(\Gamma')} \quad (2)$$

Axiom (A3): Regularity principle *Let us denote by $D(x, r)$ the disc with center x and radius r . Let $Q : \mathbb{R}^2 \rightarrow S^1$ such that there exists a parameterisation ϕ such that*

$$\phi(Q)(y) = \frac{1}{2}A_\phi(y - x, y - x) + (p_\phi, y - x) + c_\phi$$

with $A_\phi \in SM(2)$ the set of two dimensional symmetric matrices, $p_\phi \in \mathbb{R}^2$, $x \in \mathbb{R}^2$ and $c_\phi \in \mathbb{R}$. Then there exists a continuous function $F : SM(2) \times \mathbb{R}^2 \times \mathbb{R} \times \mathbb{R}^2$, independent of ϕ such that

$$\lim_{r \rightarrow 0^+} \frac{\phi(E(\partial D(x, r), Q|_{\partial D(x, r)}))(x) - \phi(Q)(x)}{r^2/2} \rightarrow F(A_\phi, p_\phi, c_\phi, x). \quad (3)$$

Axiom (A4): Translation invariance *Let $\tau_h \theta_0(x) = \theta_0(x - h)$, $\theta_0 : \mathbb{R}^2 \rightarrow S^1$, $h \in \mathbb{R}^2$. Then for all h ,*

$$E(\Gamma - h, \tau_h \theta_0) = \tau_h E(\Gamma, \theta_0). \quad (4)$$

Axiom (A5): Domain rotation invariance *For any planar rotation R ,*

$$E(R\Gamma, \theta_0 \circ R^{-1}) = E(\Gamma, \theta_0) \circ R^{-1}. \quad (5)$$

Axiom (A6): Zoom invariance Let $H_\lambda\theta_0(x) = \theta_0(\lambda x)$, for $\lambda > 0$. Then,

$$E(\lambda^{-1}\Gamma, H_\lambda\theta_0) = H_\lambda E(\Gamma, \theta_0). \quad (6)$$

Once the parameterisation is taken care of, all the results obtained in the scalar case are extended to orientation fields. This extension is nearly straightforward, complete proof can be found in [7].

Theorem 1. Assume that the interpolation operator E satisfies **(A1)**-**(A3)**. Then $F(A, p, x, c)$ does not depend on c . Moreover, if $\theta_0 \in \mathcal{F}(\Gamma)$, then $\phi(E(\Gamma, \theta_0))$ is a viscosity solution of

$$\begin{cases} F(D^2u, Du, x) = 0 \text{ in } D(\Gamma) \\ u = \phi(\theta_0) \text{ on } \Gamma. \end{cases} \quad (7)$$

Remark 1. In the scalar case [7], grey scale shift invariance is assumed to prove this result. Of course, it does not make sense for orientation fields since angles do not add. However, since the result must be invariant with respect to (w.r.t.) the parameterisation, we get an equivalent property for free.

Theorem 2. Assume that E satisfies axioms (1)-(6) and that F is differentiable at 0. Then, for all parameterisation ϕ , $\phi(E(\Gamma, \theta_0))$ is solution of

$$\begin{cases} D^2u(Du^\perp, Du^\perp) = 0 \text{ in } D(\Gamma). \\ u = \phi(\theta_0) \text{ on } \Gamma. \end{cases} \quad (8)$$

Remark that this operator is the curvature of the level lines of u , up to a $|Du|^3$ factor. These level lines are independent of the parameterisation, which makes the result possible. Indeed, the independence w.r.t. the parameterisation implies that, for all admissible ϕ and ψ ,

$$E(\Gamma, \theta_0) = \phi^{-1} \circ E_\phi(\Gamma, \phi \circ \theta_0) = \psi^{-1} \circ E_\psi(\Gamma, \psi \circ \theta_0).$$

By noting $u = \phi \circ \theta_0$ and $g = \psi \circ \phi^{-1}$, this equation becomes

$$g \circ E_\phi(\Gamma, u) = E_\psi(\Gamma, g \circ u).$$

This condition is closely related to invariance with respect to contrast change for scalar data, and the arguments developed in [1] indeed apply.

As noted in disocclusion experiments [18], this operator interpolates the level lines of the data with straight lines. A well known problem is that the solution of this equation may not be unique, and as shown in Section 6 that if it manages to keep the discontinuities structuring the image, it fails to give a field smooth enough to recover subjective contours. Thus we may drop the full independence w.r.t the parameterisation and slightly relax Axioms (1) and (3).

Proposition 2. *Assume that Axioms (1) and (3) only holds for parameterisation that are Euclidean, up to a multiplicative factor. Then $\phi(E(\Gamma, \theta_0))$ is solution of*

$$aD^2u(Du, Du) + bD^2u(Du, Du^\perp) + cD^2u(Du^\perp, Du^\perp) = 0, \quad (9)$$

where $ac - b^2 \geq 0$.

Condition $ac - b^2 \geq 0$ ensures that the equation is elliptic, and that the maximum principle holds. As expected, a solution of (9) is invariant with respect to an affine reparameterisation of the circle, but not to any general parameterisation.

Among all those operators, the case $b = c = 0$ is the Absolutely Minimizing Lipschitz Extension (AMLE)

$$\begin{cases} D^2u(Du, Du) = 0 \text{ in } D(\Gamma), \\ u|_\Gamma = \phi(\theta_0) \text{ on } \Gamma, \end{cases} \quad (10)$$

for which existence and uniqueness of viscosity solution are known. It gives continuous oscillation free solution. It is studied in more detail in Sect. 4.2.

4 Two Interpolation Operators

4.1 Angle Interpolation with the Curvature Operator

As a result of the previous section, the only operator satisfying the given axioms is the curvature operator. It is well known in the computer vision community as a scalar restoration operator via total variation minimisation and has been used for scalar interpolation to solve the disocclusion problem [9, 18, 27].

The argumentation above gives the equation which is locally satisfied by the orientation of the vector field. An alternate formulation [30] is to consider the variational problem

$$\min_{W^{1,p}(\Omega)} \int \|DI\|^p,$$

under the constraint $|I| = 1$. In this case $I = (I_1, I_2)$ and $|I|$ is the Euclidean norm $|I| = \sqrt{I_1^2 + I_2^2}$ and $\|DI\| = \sqrt{|DI_1|^2 + |DI_2|^2}$. Inspired by the scalar case, we can compute the Euler-Lagrange equations for the energy above by setting $I = \frac{u}{|u|}$ so that the constraint is automatically satisfied. Careful calculations lead to a system of the two coupled PDEs

$$\operatorname{div} (\|DI\|^{p-2} DI_i) + I_i \|DI\|^p = 0, \quad 1 \leq i \leq 2. \quad (11)$$

It is worth noticing that $\|DI\|^p$ may be interpreted as the Lagrange multiplier of the constraint $|I| = 1$. The case $p = 1$, corresponding to the total variation, leads to

$$\operatorname{div} \left(\frac{DI_i}{\|DI\|} \right) + I_i \|DI\| = 0, \quad 1 \leq i \leq 2. \quad (12)$$

As a sanity check, elementary calculations lead to the following result, which holds thanks to the particular choice of norm $\|DI\|$.

Proposition 3. *Let $I = (I_1, I_2) \in C^2(\Omega, \mathbb{R}^2)$ with $|I| = 1$ everywhere. Let θ such that $I = (\cos(\theta), \sin(\theta))$. Then*

$$\operatorname{div} \left(\frac{DI_i}{\|DI\|} \right) + I_i \|DI\| = 0, \quad 1 \leq i \leq 2. \iff \frac{1}{|D\theta|} D^2\theta \left(\frac{D\theta^\perp}{|D\theta|}, \frac{D\theta^\perp}{|D\theta|} \right) = 0. \quad (13)$$

Thus minimizing the L^1 norm of the gradient of a vector field of \mathbb{R}^2 constrained on the unit circle is equivalent to solving the unconstrained intrinsic equation on angle.

4.2 AMLE on angle

In this section, more insight on the AMLE extension is provided. A more detailed presentation can be found in [3, 7, 15]. We know that a non surjective data can be smoothly interpolated inside a single parameterisation, and that AMLE is independent of affine change of parameterisation.

AMLE was introduced in [2]. It was proved (see [3, 15] and references therein) that it can be equivalently defined, in the scalar case, as

- the extension in Ω of a data defined on $\partial\Omega$ whose Lipschitz constant is minimal in any $\Omega' \subset \Omega$.
- the viscosity solution of the PDE $D^2u(Du, Du) = 0$.
- the limit for $p \rightarrow \infty$ of p -harmonic maps, defined as the minimization of the p -harmonic energy

$$\min_{W^{1,p}(\Omega)} \int |Du|^p.$$

Those results heavily rely on a maximum principle (eventually proved by Jensen [15]), which guarantees that the solution has no oscillation inside the domain. More importantly, it yields the existence and uniqueness of the solution.

Again, the intrinsic formulation on angle used until now and the \mathbb{R}^2 restricted to S^1 one can be linked. Let us consider (11) again and let p go to $+\infty$. We formally obtain the two coupled equations

$$\sum_{i=1}^2 D^2 I_i(DI_i, DI_j) = 0 \quad j = 1, 2. \quad (14)$$

The definition of a solution of this system is, to the best of our knowledge, an open problem. However, we point out the two following interesting facts.

Proposition 4. *Let $I = (I_1, I_2) \in C^2(\Omega, \mathbb{R}^2)$ with $|I| = 1$ everywhere. Let θ such that $I = (\cos(\theta), \sin(\theta))$. Then*

$$\sum_{i=1}^2 D^2 I_i(DI_i, DI_j) = 0 \quad j = 1, 2 \iff D^2\theta(D\theta, D\theta) = 0. \quad (15)$$

This means that I is a vector AMLE on the circle if its argument is a scalar AMLE. As the solution of the scalar equation is unique, we can say that if a C^2 solution of the vector equation exist, it is unique.

The second point is that the term corresponding to the constraint $|I| = 1$ has vanished from (11) to (14). Now, a method to solve the stationary problem (14) is to solve the corresponding evolution system

$$\frac{\partial I_j}{\partial t} = \sum_{i=1}^2 D^2 I_i(DI_i, DI_j) \quad j = 1, 2. \quad (16)$$

In the scalar case, it is known that it converges as $t \rightarrow \infty$ to the unique solution of the stationary problem. Thanks to Proposition 4, this result is still valid for C^2 solution of the vector problem (14).

If I is a solution of (16) such that $|I| = 1$ everywhere at time $t = 0$, does it remain true for $t > 0$? At this step, we cannot tell, but we have the following hint.

Lemma 1. *Let I be a C^2 vector field with $|I| = 1$ everywhere. Then the vector with coordinates $\sum_{i=1}^2 D^2 I_i(DI_i, DI_j)$ is everywhere normal to I .*

Proof. Let $F_j = \sum_{i=1}^2 D^2 I_i(DI_i, DI_j)$, $j = 1, 2$. We can write $F_j = DI_j \cdot D(|DI|^2)$, $j = 1, 2$. Thus,

$$I \cdot F = (I_1 DI_1 + I_2 DI_2) \cdot D(|DI|^2) = I^t DI \cdot D(|DI|^2),$$

with DI the 2x2 matrix defined by the column (DI_1, DI_2) . On the other hand, by derivation of the constraint $|I|^2 = 1$, we have $D(|I|^2) = 0$, and we can write:

$$D(|I|^2) = D(I \cdot I) = D(I^t I) = 2I^t DI$$

Thus $I^t DI = 0$, and $I \cdot F = 0$. □

5 Numerical resolution

The numerical implementation of the two singled out operator is carried out using their time dependent gradient flow equation:

$$\frac{du}{dt} = F(Du, D^2u), \quad (17)$$

letting $t \rightarrow \infty$. In the standard scalar cases, it is known that it converges as $t \rightarrow \infty$ to the solution of the stationary equation. There is no such result in our case, but the experiments show that it is a reasonable assumption. We solved numerically the intrinsic scalar equations, the implementation were done using the Megawave2 software [13]. The equivalences with vector formulation we stated earlier are indeed experimentally verified by numerical result not shown here.

A numerical analysis of scalar AMLE showing a convergent difference scheme is available in [22]. It is based on the maximum principle, hence it works well if the data verifies the condition (C) but fails completely in the general case. Indeed S^1 lacks a global order relation and a scheme based on a global maximality principle is bound to fail. In [7], a had-hoc non-linear over relaxation scheme (NLOR) to solve scalar AMLE is used. A similar scheme is exploited here.

In addition, due to the intrinsic periodicity of angular data, specific issues have to be dealt with: some numerical attention have to be taken, and as underlined in Section 2, a multiresolution scheme is needed to solve the problem of initialisation.

5.1 Finite Differences Schemes

5.1.1 Numerical Scheme

The non-linear over relaxation scheme (NLOR) we present here is essentially similar to [7]. Equation system 17 is discretized by an Euler implicit scheme

$$u_{i,j}^{n+1} = u_{i,j}^n + \Delta t(F(D^2 u_{i,j}^{n+1}, Du_{i,j}^{n+1})), \quad (18)$$

Let x_i , $i = 1, k$ be the $k = 2N^2$ unknown $(u_{i,j}^{n+1}, v_{i,j}^{n+1})_{i,j \in [1 \dots N]}$ of that system of k equations. It can be written as

$$f_p(x_1, x_2, \dots, x_k) = 0 \quad p = 1, \dots, k. \quad (19)$$

The idea of NLOR is to introduce a parameter ω and to iteratively compute, at each time step

$$x_i^{n+1} = x_i^n - \omega \frac{f_i(x_1^{n+1}, x_2^{n+1}, \dots, x_{i-1}^{n+1}, x_1^n, x_2^n, \dots, x_k^n)}{f_{ii}(x_1^{n+1}, x_2^{n+1}, \dots, x_{i-1}^{n+1}, x_1^n, x_2^n, \dots, x_k^n)} = 0 \quad i = 1, \dots, k, \quad (20)$$

with $f_{ii} = \frac{\partial f_i}{\partial x_i}$.

As stressed in Section 4.2, this equation preserves the norm. However, due to the addition of numerical approximation at each time step, that condition is not actually fulfilled. Consequently, as in [30] a projection on S^1 step have been added at each iteration : the correction is always very small and it ensure convergence.

5.1.2 Numerical problem constrained in S^1

As noted in [26], working with angle modulo 2π demands special numerical attention to circumvent the problem caused by the discontinuities at $2k\pi$, $k \in \mathbb{N}$. In [26] it has been proposed to approximate θ by $\sin(\theta)$, thanks to the Taylor formula $\sin(\theta) = \theta + O(\theta^3)$; however, this method loses accuracy when $|D\theta|$ is high. These problems have also been investigated in [8], in which the two following workarounds are proposed.

The first is the *adaptive Riemann surface method*, in which one chooses at each stencil point the value of k minimizing $|(\theta_{i-1,j} + 2k\pi) - \theta_{i,j}|$ (for example for a two points first order finite difference in \mathbb{R}^2). The second method is a *multiple parameterisation method*, in which at each point the data is rotated such that there is no discontinuity in the region where the finite difference is being computed. In the following a variant of the adaptive Riemann surface method is used, replacing $\theta - \tilde{\theta}$ in \mathbb{R} by $\theta - (\tilde{\theta} + k\pi)$, $k = \operatorname{argmin}(\tilde{\theta} - k\pi)$ in $\mathbb{R}/2\pi\mathbb{Z}$.

5.2 A Multiresolution Initialisation Method

As stated in Section 2.2, due to a fundamental ambiguity in angle interpolation and the iterative nature of the numerical scheme, initialisation plays an important part. Its importance is even greater in the curvature case, as no unicity result is available even in the scalar case. The chosen solution is a multi-resolution scheme, with a bottom-up data construction part, and a top-down computation part as illustrated Fig. 2.

The aim of the bottom-up step is to compute an initialisation value for each point to be interpolated: from a given resolution to the next, the number of lines and columns of the initial data image are divided by two, and each pixel of the coarser superior resolution is filled with the average of the four corresponding pixels of the inferior resolution. Thus even if three of those four points are unknown, the corresponding pixel of the next resolution will be set, so that at the last resolution all the pixels are known.

From there begins the top-down calculus part, which computes the AMLE at each resolution beginning from the top. The coarser resolution is by construction fully known, and from there on the computations at a given resolution are initialised with the projection from the resolution above it. So in the end a given unknown point is initialised the first time it appear in the pyramid by the average of the nearest known points.

6 Numerical Experiments

6.1 Experiments on the curvature operator

Geometrically, the curvature extension operator tries to extend the level lines of the boundary data by straight lines. Obviously, there are cases for which that approach does not apply [18]. In particular it fails to compute any solution for the simple artificial cases presented in the next section (see figure 4).

However, experiments carried out for larger images with a larger set of boundary points yields interesting results. Figure 3 displays an example with the Lena image. The field is visualised via its field line, using Line Integral Convolution (LIC) [5]. The initial field is given by the orientation of the tangents to the level lines (the orthogonal to the gradient) decimated with a thresholded Canny-Deriche edge filter [11] (Megawave2 implementation [13]). As expected,

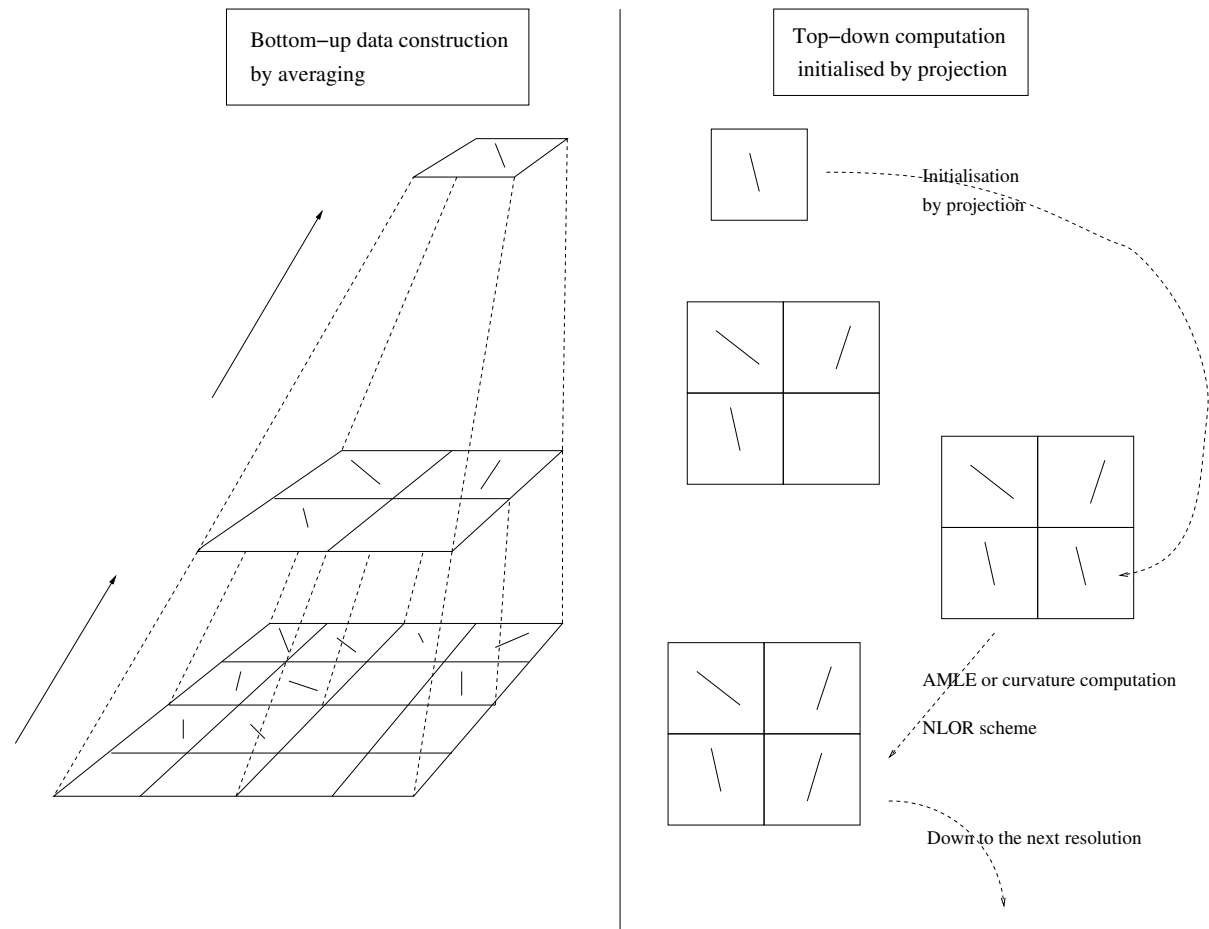


Figure 2: Multiscale scheme: a given point to be interpolated is initialised with the average of it's nearest neighbour.

the curvature operator keeps discontinuities, as at the top of Lena’s hat. Interestingly, it also manages to keep singularities adequately. In particular, *T-junctions* are preserved, which is particularly relevant from a perceptual point of view. Not only singularities that are present on the boundary data are preserved, but they can also be created in the interpolated area in a suitable way (see for instance at the interface of the cheek and the hair).

To sum up, the curvature operator is (as in the scalar case) able to preserve singularities when necessary. It may be considered as a drawback when the smoothest solution is sought. Moreover, there is no existence and uniqueness result in the general case.

6.2 Experiments on the AMLE Operator

Figure 4 shows numerical results on artificial data. The first one simply consists of two vectors. The interpolated vector field is as expected tangent to the curve with which we would like to connect the two vectors, something close to Euler elastica [21]. The next two figures show the same mechanism with more complex curves: a circle and a tube. The interpolated field is perceptually sound.

As asserted by Prop. 1, we do find singularities in the center of the circle and the extension is there somewhat chaotic, as we are looking for a Lipschitz function where it cannot even be continuous. The situation below the tube (Fig. 4, last experiment) is interesting as it is an example of the ambiguity of Sect. 2.2: a smooth extension does exist, but due to the lack of information the algorithm extends the orientation field the other way round and puts a singularity.

An experiment on Lena is reported Fig. 5. The initial field is again the orientation of the tangents to the level lines (the orthogonal to the gradient) decimated with a thresholded Canny-Deriche edge filter [11]. The interpolation field is again tangent to the edges as requested. On the other hand, there is no control on the position of the unavoidable singularities. Moreover, singularities are smoothed out, which can be expected, regarding the properties of the AMLE in the scalar case.

Nonetheless, the AMLE is a good candidate for an interpolation operator as we have a complete theory in the scalar case stating existence and uniqueness of solution. Moreover, it gives smooth solution from which extracting subjective contour as curves is possible. Compared to the curvature however, it tend to lack the ability to keep discontinuities in the fields it produce.

7 Applications

This section present two applications of the AMLE interpolation operator. Its faculty of continuously extending extracted geometrical information in images is used to find edge curves and smooth highly structured images.



Figure 3: Interpolation with the curvature operator on Lena. The initialization is orthogonal to the gradient orientation field decimated using a Canny-Deriche filter. A general observation is that T-junctions are preserved.

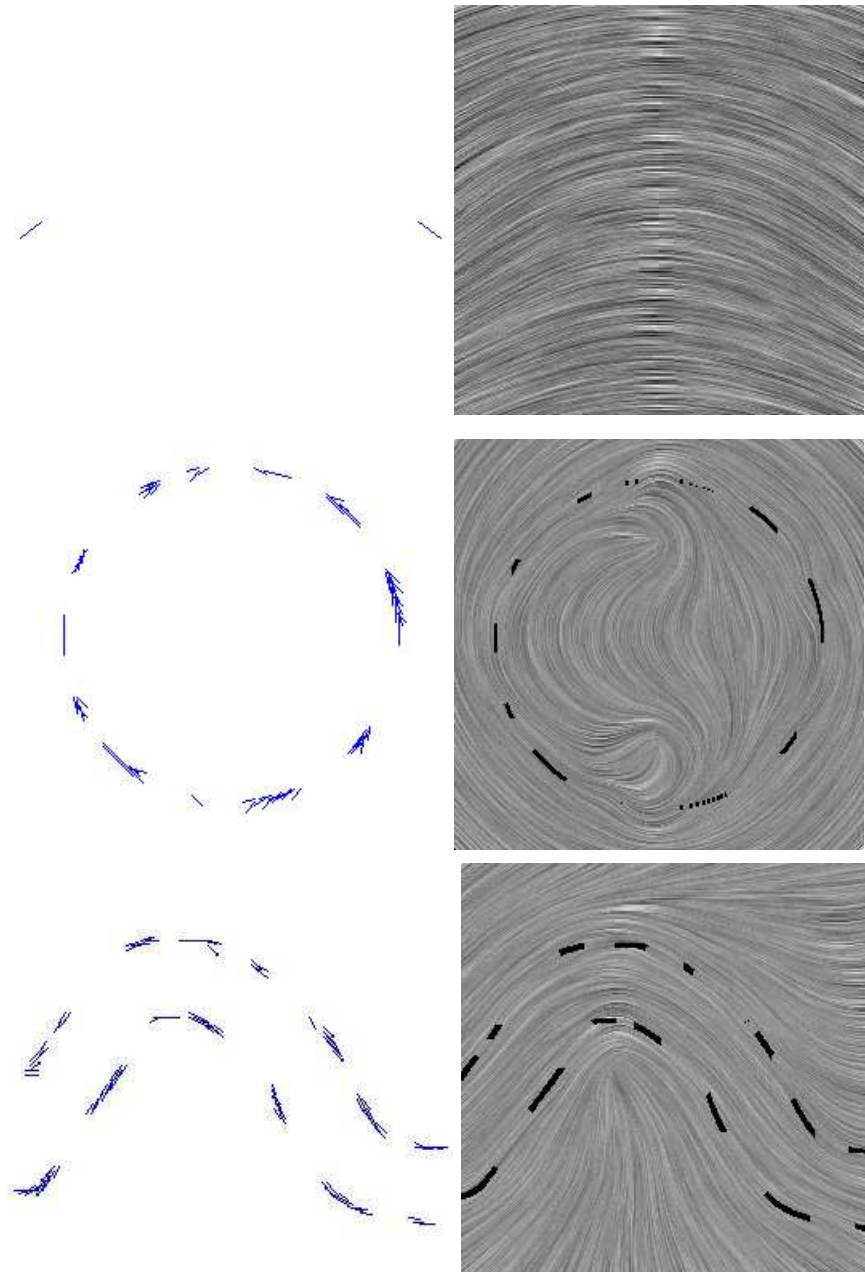


Figure 4: Three artificial geometric tests, initial orientation field on the left, AMLE extension visualised with LIC on the right. The computed field recovers the curves from which the initial data were extracted. Outside of them its behaviour is less predictable.



Figure 5: Test with the Lena image, initialised with the orthogonal to the gradient orientation field decimated using a Canny-Deriche filter. Notice that the recovered field is tangent to the edges, in particular at the top of the hat, on the strands of hair around the face and on Lena's jaw and chin.



Figure 6: A detail of a Henri Cartier-Bresson photo (in Srinagar, Kashmir, 1948). Left: original and extracted point to be interpolated. Right: up AMLE extension and down curvature extension.

7.1 Extracting Curves from Orientation Field as Geodesics

We now are provided with a smooth orientation field θ , extending some extracted data. Let us assume that those initial orientations can be considered as edgels, i.e. they are tangent to an edge. The continuous field computed by AMLE is then assumed to be tangent to the full edge the initial edgels are part of. Thus, given two points linked by a geometrical structure in the original image, that structure can be looked for as the line *as tangent as possible* to θ that joins them.

Using minimal path formulation [10], given two point M_0 and M_1 and vector field u the extraction of the looked after curve Γ_{M_0, M_1} is stated as minimizing a given metric $F(u, \Gamma)$. Let us set $E_{F(u, \Gamma)}(M_0, M_1) = \int_{M_0}^{M_1} F(u, \Gamma)$. The curve Γ_{M_0, M_1} is defined by $\Gamma_{M_0, M_1} = \arg \min_{\tilde{\Gamma} \in \mathcal{C}(M_0, M_1)} E_{F(u, \tilde{\Gamma})}(M_0, M_1)$, with $\mathcal{C}(M_0, M_1)$ the set of continuous curves from M_0 to M_1 . To solve for it, we compute

$$E_{M_0}(x) = \min_{\tilde{\Gamma} \in \mathcal{C}(M_0, x)} E_{F(u, \tilde{\Gamma})}(M_0, x)$$

for all $x \in \Omega$. $E_{M_0}(x)$ is a convex function whose only minimum is in M_0 , thus it leads to Γ_{M_0, M_1} by a simple gradient descent on E_{M_0} from M_1 to M_0 . To actually compute E_{M_0} , the Fast Marching algorithm [28] is used. It is based on a front propagation of equation

$$\frac{\partial C}{\partial t}(\lambda, t) = \frac{1}{F(u, \Gamma_{M_0, C(\lambda, t)})} \mathbf{n}(C(\lambda, t)), \quad (21)$$

with C the front, initially an infinitesimal circle around M_0 , λ an euclidean parameterisation of C and \mathbf{n} the outward normal to the front. $E_{M_0}(x)$ is then defined as the arrival time of the front at each point. Thus at any given time, minimal paths have been computed from M_0 to all the points already visited by the front at that time, they can then be used to further propagate it.

The proposed function F is

$$F(u, \Gamma)(y) = \left(\frac{\partial \Gamma(\lambda)}{\partial \lambda}(y), u^\perp(y) \right)^2,$$

with λ an Euclidean parameterisation of Γ , u^\perp the orthogonal of u and (\cdot, \cdot) the usual scalar product of \mathbb{R}^2 . It is by definition null if u is tangent to Γ and maximum if it is orthogonal. This function F can be considered as the only parameter for the edge extraction.

In Figures 7(a) and 7(b), the results for real images are displayed. On the Lena image (Fig. 7(a)), using the field computed as per section 4.2, we have recovered the top of the hat and the left jaw, which both were not contrasted enough to be extracted by our point-wise thresholded edge extraction filter. This is a typical case of modal completion, also called illusory contour, where the background and the edge have in part the same color. Figure 7(b) shows two examples of images with low contrast: in both cases the presence of a structure is clearly recognized while continuous contours or edges are either very faint or

not actually present. Thus the use of orientation informations allow us to tackle problem on which method purely based on image intensity would encounter difficulties.

7.2 Smoothing Along Orientation

In [31] is described an anisotropic smoothing algorithm based on the Line Integral Convolution (LIC) of Cabral and Leedom [5]. Given an image I_0 and a vector field u , if Γ_x is the integral line of u going through x with λ an euclidean parameterisation of Γ_x , the unidimensional heat equation constrained on the integral curves of u ,

$$\forall x \in \Omega \quad \frac{\partial I(\Gamma_x(\lambda))}{\partial t}(x) = \frac{\partial^2 I(\Gamma_x(\lambda))}{\partial \lambda^2}(x), \quad (22)$$

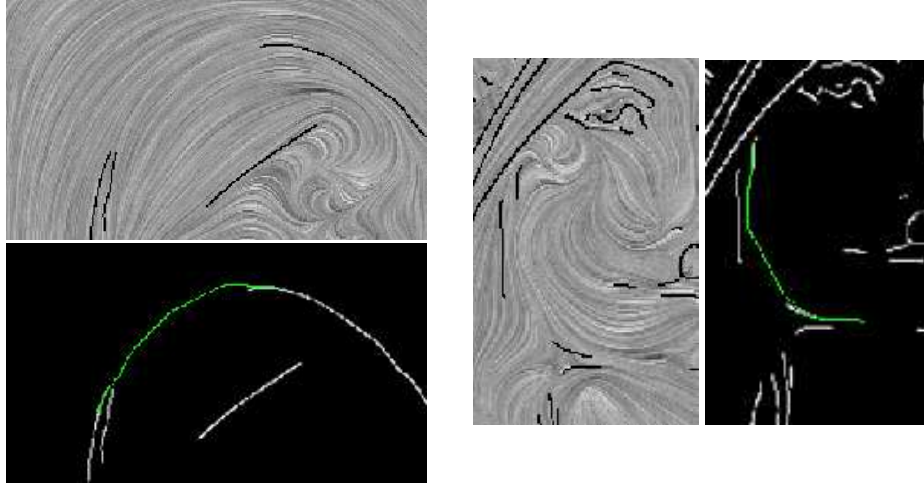
is equivalent to a trace based differential operator on the full image. As it is well known that heat equation is equivalent to a Gaussian convolution, (22) is in turn equivalent to

$$\forall x \in \Omega \quad I(t)(x) = \int_{-\infty}^{+\infty} I_0(\Gamma_x(\lambda))G_t(\lambda)d\lambda, \quad (23)$$

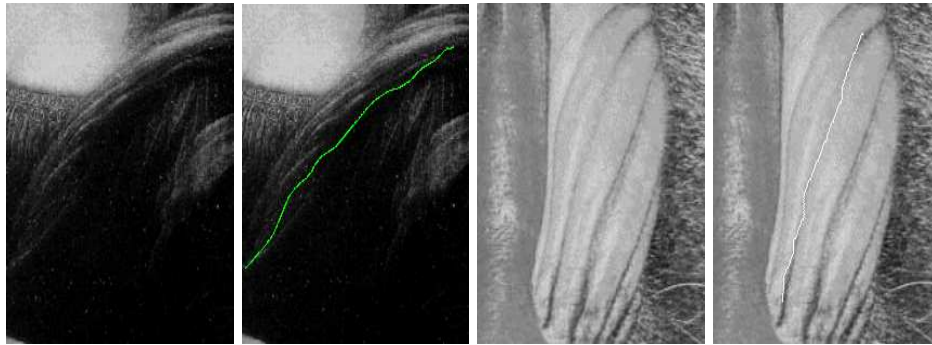
with G_t the Gauss function of standard deviation \sqrt{t} : $G_t(x) = \frac{1}{\sqrt{4\pi t}} \exp(-\frac{x^2}{4t})$. This is the continuous formulation of the LIC visualization algorithm [5], which is used to visualize the vector fields in this paper.

In [31], the local geometrical information of the image was captured into a diffusion tensor based on the structure tensor [32] which was decomposed into vectors to apply the described LIC-based regularisation. While in the general case a vector field would be an appropriate description of an image only on edges (see section 7.1), in some particular cases it might describe the whole image. Images displayed in Fig. 7(c) are accurately described by a set of linear or curvilinear parallel lines. In those cases, an orientation field computed by the AMLE operator over suitably extracted point might be an accurate description of the image. Such a field is computed and used to implement the LIC-based regularization defined by Eq. 23.

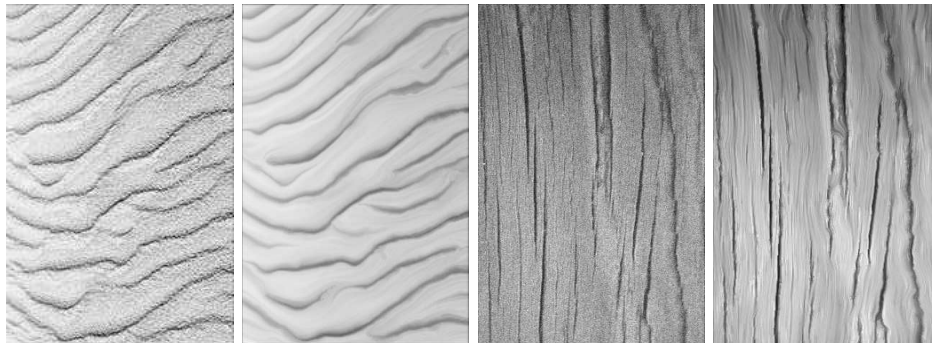
The image in the left part of Figure 7(c) is a patch of sand. This is a natural image with no artificial noise, and the geometry of the image underlying its grainy natural aspect is recovered. On the right is a wood texture image with Gaussian noise of standard deviation 20 added. It exhibits vertical cracks, which are captured in the computed orientation field. As illustrated, the orientation based filtering leads to an efficient restoration. Thus, when strong geometrical structures are available, the use of such orientation fields is an elegant and intuitive alternative to the diffusion tensor [31].



(a) Edge extraction on the lena image (detail). For both curves: the computed AMLE along with the initialisation points visualised with LIC, and the same extracted point with the extracted curve on top.



(b) Two example of curve extraction in poorly contrasted image part, left Da Vinci's Mona Lisa scarf, right a detail of the baboon image.



(c) Left: sand patch, left original image (no noise added), right LIC-smoothed version using the orientation field computed as per Sec. 4.2 (not shown), right: wood texture image, left original (with Gaussian noise $\sigma = 20$) and right LIC-smoothed.

8 Conclusion

An axiomatic approach of orientation field interpolation has been presented to define extension operators. There is a unique operator satisfying a small set of axioms including geometrical invariance and stability: the curvature operator. This operator is able to preserve singularities. On the other hand, one may require a smoother solution. Moreover, existence and uniqueness of a solution are not well established. If the independence of the interpolation with respect to reparameterisation of the unit circle is relaxed, another operator becomes interesting: the AMLE. Existence and uniqueness holds in the scalar case. The AMLE is, to some extent, dual to the curvature operator (it minimizes the L^∞ norm of the gradient, while the curvature minimizes the norm L^1), and somehow smoothes out the singularities.

Those operators are the more natural popping out from the required axioms. However, if some of them are relaxed or more prior knowledge from the image is introduced, some variations of these operators may lead to new types of interpolation model.

Two applications of the AMLE operator were shown, which take advantage of its faithful and continuous interpolation of edgels to extract curves in poorly contrasted image part and drive a purely geometric smoothing method. The curvature operator, while being more pleasant to the human eyes because of its ability to keep structuring discontinuity has proved harder to use in such relatively simple method. This is due to the lack of uniqueness, which allow for very different solution according to the initialisation. The presented multi-resolution initialisation process is a first step towards a solution to that problem.

Beyond more advanced edge extraction algorithm, practical use of the presented algorithm include processing and analysis of strongly organised images. These include biological images like fish otoliths (small stones used for spatialisation), shells of seashells, or corals, that show peculiar seasonal concentric structures. They are of importance because of their use in ecological studies [24], e.g. age-based fish stock assesment or paleoclimatology.

References

- [1] L. Alvarez, F. Guichard, P. L. Lions, and J.M. Morel. Axioms and fundamental equations of image processing. *Arch. Rational Mechanics and Anal.*, 16(IX):200–257, 1993.
- [2] G. Aronsson. Extention of function satisfying lipschtiz conditions. *Ark. Mat.*, 6:551–561, 1967.
- [3] G. Aronsson, M. G. Crandall, and P. Juutinen. A tour of the theory of absolutely minimizing functions. *Bull. Amer. Math. Soc.*, 41:439–505, 2004.
- [4] C. Ballester, V. Caselles, and J.Verdera. Disocclusion by joint interpolation of vector fields and gray levels. *Multiscale Modelling and Simulation*, 2(1):80–123, 2003.

- [5] B. Cabral and L. C. Leedom. Imaging vector fields using line integral convolution. In *SIGGRAPH '93: Proceedings of the 20th annual conference on Computer graphics and interactive techniques*, pages 263–270, 1993.
- [6] V. Caselles, R. Kimmel, and G. Sapiro. Geodesic active contours. *Int. J. Computer Vision*, 22(1):61–79, 1997.
- [7] V. Caselles, J.M. Morel, and C. Sbert. An axiomatic approach to image interpolation. *IEEE Trans. Image Processing*, 7(3):376–386, 1998.
- [8] T. Cecil, S. Osher, and L. Vese. Numerical methods for minimization problems constrained to S^1 and S^2 . *J. of Computational Physics*, 198(2):567–579, 2004.
- [9] T. Chan and J. Shen. Local inpainting model and TV inpainting. *SIAM J. Appl. Math.*, 62(3):1019–1043, 2001.
- [10] Laurent D. Cohen. Minimal paths and fast marching methods for image analysis. In Nikos Paragios, Yunmei Chen, and Olivier Faugeras, editors, *Mathematical Models in Computer Vision: The Handbook*. Springer, 2005.
- [11] R. Deriche. Using canny’s criteria to derive a recursively implemented optimal edge detector. *Int. J. Computer Vision*, 1(2):167–187, 1987.
- [12] A. Desolneux, L. Moisan, and J.M. Morel. Edge detection by helmoltz principle. *J. Math. Imaging and Vision*, 14(3):271–284, 2001.
- [13] J. Froment. Megawave2. <http://www.cmla.ens-cachan.fr/Cmla/Megawave/>.
- [14] A. Granas and J. Dugundji. *Fixed point theory*. Springer-Verlag, 2003.
- [15] R. Jensen. Uniqueness of lipschitz extentions: minimizing the sup norm of gradient. *Arch. Rational Mechanics and Anal.*, 123:51–74, 1993.
- [16] G. Kaniza. *La grammaire du voir*. Diderot, 1996.
- [17] R. Kimmel and N. Sochen. Orientation diffusion or how to comb a porcupine. *Journal of Visual Communication and Image Representation*, 13(1):238–248, 2002.
- [18] S. Masnou and J.M. Morel. Level-line based disocclusion. In *IEEE International Conference on Image Processing*, pages 259–263, Chicago, USA, October 1998.
- [19] G. Medioni and M.S. Lee. Grouping $\cdot, -, \dot{\cdot}$ into regions, curves, and junctions. *Computer Vision and Image Understanding*, 76(1):54–69, 1999.
- [20] G. Medioni, M.S. Lee, and C.K. Tang. *A computational framework for segmentation and grouping*. Elsevier Science, 2000.

- [21] D. Mumford. Elastica and computer vision. In Chandrajit Bajaj, editor, *Algebraic Geometry and Its Applications*, pages 491–506. Springer-Verlag, 1994.
- [22] A.M. Oberman. A convergent difference scheme for the infinity laplacian: construction of amle. *Math. Comp.*, 74(251):1217–1230, 2004.
- [23] S. Osher, A. Sole, and L. Vese. Image decomposition and restoration using total variation minimization and the H^1 norm. *Multiscale Modeling and Simulation*, 1(3):349–370, 2003.
- [24] J. Panfili, H. de Pontual, H. Troadec, and P.J. Wright, editors. *Manual of fish sclerochronology*. Ifremer-ird coedition, 2002.
- [25] P. Parent and W. Zucker. Trace inference, curvature consistency, and curve detection. *IEEE Transactions on Pattern Analysis and Machine Intelligence*, 11(8):823–839, 1989.
- [26] P. Perona. Orientation diffusion. *IEEE Trans. Image Processing*, 7(3):457–467, 1998.
- [27] L. I. Rudin, S. Osher, and E. Fatemi. Nonlinear total variation bsaed noise removal algorithms. *Physica D*, 60:259–268, 1992.
- [28] J.A. Sethian. *Level Set Methods and Fast Marching Methods*. Cambridge University Press, 1999.
- [29] A. Sha’ashua and S.Ullman. Structural saliency: The detection of globally salient structures using a locally connected network. In *Second Int. Conf. Comp. Vision, Tarpon Springs, FL*, pages 321–327, 1988.
- [30] B. Tang, G. Sapiro, and V. Caselles. Diffusion of general data on non-flat manifolds. *Int. J. Computer Vision*, 36(2):149–161, 2000.
- [31] D. Tschumperlé. LIC-based regularization of multi-valued images. In *IEEE International Conference on Image Processing*, pages 533–536, Genoa, Italy, 2005.
- [32] J. Weickert. *Anisotropic Diffusion in Image Processing*. Teubner-Verlag, Stuttgart, 1998.
- [33] M. Wertheimer. Untersuchungen zur Lehre der Gestalt II. *Psychologische Forschung*, 4:301–350, 1923.
- [34] J. Zweck and L.R. Williams. Euclidian group invariant computation of stochastic completion fields using shifttable-twistable basis function. *J. Math. Imaging and Vision*, 21(2):135–154, 2004.